



A shortcut from broadband to spectral aerosol optical depth

Martin Kannel^{a*}, Hanno Ohvril^a, and Oleg Okulov^b

^a Institute of Physics, University of Tartu, Ülikooli 18, 50090 Tartu, Estonia

^b Estonian Meteorological and Hydrological Institute, Mustamäe tee 33, 10616 Tallinn, Estonia

Received 29 March 2011, revised 2 April 2012, accepted 27 April 2012, available online 20 November 2012

Abstract. The concept behind the shortcut idea is a close correlation between column broadband aerosol optical depth (BAOD) and aerosol optical depth at 500 nm (AOD500). The method uses only two input parameters: (a) the Bouguer broadband coefficient of column transparency for optical mass $m = 2$ (solar elevation about 30°) and (b) integrated column precipitable water vapour which can be roughly estimated using surface water vapour pressure. In creating the method, a large database, including almost 20 000 complex, spectral and broadband direct solar beam observations at Tõravere, Estonia, during all seasons of a 8-year period, 2002–2009, was used. The AOD500 observations were performed by the NASA project AERONET and the broadband direct beam ones by the Estonian Meteorological and Hydrological Institute. Analysis of this database revealed a high correlation between BAOD and AOD500 which enabled transition from broadband to spectral AOD. Almost 82% of the observations in the database belonged to lower turbidities when $\text{AOD500} < 0.2$. The root mean square deviation (RMSD) for AOD500 prediction in this range was 0.022. For $\text{AOD500} = 0.2\text{--}0.4$, the RMSD was 0.035, for $0.4\text{--}0.6$, the RMSD was 0.042. Relative RMSD for these ranges was about 22%, 12%, and 9%, respectively. For $\text{AOD500} > 0.6$, relative RMSD remained 9%. For comparison, the same database was used to test Gueymard's broadband parameterization based on his SMARTS2 classic model. The last one, apparently due to problems with circumsolar radiation, slightly but systematically underestimated the AOD500. However, there was a close correlation between our shortcut results and Gueymard's broadband parameterization.

Key words: AERONET, aerosols, aerosol optical depth, light attenuation, atmospheric integral transparency coefficient, broadband direct irradiance.

1. INTRODUCTION

Spectral aerosol optical depth of the atmospheric column, or extinction coefficient due to aerosol particles, $\text{AOD}\lambda$, is a central quantity in optics of atmospheric aerosols. It is usually measured with a multispectral instrument, sunphotometer, at a number of wavelengths, commonly including $\lambda = 500$ or 550 nm. There are two reasons for the $\text{AOD}\lambda$ use. First, this parameter informs about turbidity of the atmospheric column. Second, dependence of $\text{AOD}\lambda$ on wavelength λ is inversely related to size distribution of aerosol particles.

Due to high initial cost sunphotometers are expensive to obtain. Also their maintainance, because of regular servicing, is expensive – annual filter changing and recalibration at mountain locations with cloudless sky, at high Sun and very clear, stable atmosphere. For

that reason, the net of sunphotometers was sparse until the end of the 1990s. The situation changed completely with the advent and expansion of the NASA huge AERONET project providing the scientific community with massive high-quality standardized global surface information on $\text{AOD}\lambda$ (Holben et al., 1998). It should be underlined that until now, the AERONET information is free to download. Like several other global atmospheric projects – NAAPS, HYSPLIT, MODIS, etc. – the free use of data is generously funded by the US government and tax-payers.

However, there are strong reasons to continue elaboration of alternative, mainly broadband evaluations for $\text{AOD}\lambda$. An example of this kind of necessity is retrospective (or prospective) retrieval of $\text{AOD}\lambda$ for periods in the past (or future) decades when spectral measurements were not (or will not be) available. Another example is a quick $\text{AOD}\lambda$ estimation for correction of satellite remotely sensed data for regions

* Corresponding author, martin.kannel@ut.ee

where spectral solar observations are not available but the broadband ones are.

Sometimes, during a later inspection of time series of AOD λ , the recorded data seem too large (overestimated) for a certain period. As usual in solar radiation observations, a doubt arises about an undesirable object (insect, spider's thread, trash, etc.) dwelling on or inside the instrument's tube. When there was only one sunphotometer operating but at the same time broadband direct beam was also recorded, an alternative AOD λ estimation, through broadband approach, makes available reliability evaluations of spectral observations.

And obviously, sites, which have enjoined a free use of AERONET observations without starting up their own solar spectral instrumentation, should be prepared to decrease in the number of simultaneously monitoring autonomous photometers or even general completion or commercialization of the AERONET project.

In Estonia, the AERONET CIMEL photometer began observations on 3 June 2002, at Tõravere (58°15', 26°27', 70 m ASL), on the territory of the Tartu–Tõravere Meteorological Station. The station is included into the Baseline Surface Radiation Network (Kallis et al., 2005). Simultaneous registration of both spectral and broadband irradiances provided the opportunity to create a joint, integrated database for AOD λ and broadband parameters of atmospheric transparency (turbidity). For eight years, 2002–2009, our joint database includes 19 592 spectral-broadband solar direct irradiance and surface water vapour pressure observations. About 75% of observations were made in April, May, June, July, and August, 9% in September, 8% in March, 3.6% in October, and only 4.4% together in January, February, and November. Due to low Sun and calibrations no joint observations were made in December.

We consider a slant atmospheric column with optical mass $m = 2$ (solar elevation $\approx 30^\circ$), consisting of three successive layers: (a) an ideal, clean, and dry atmosphere which includes O₃ and NO₂; (b) water vapour; and (c) aerosol particles. This consideration enables us to express extinction of the broadband direct beam using a product of individual transmittances of each layer and to calculate, as a residual term, broadband aerosol optical depth, BAOD2, at $m = 2$, for each of the 19 592 joint observations. The plot of the obtained values of BAOD2 against AOD500 revealed a high parabolic correlation enabling a “shortcut” from AOD500 to BAOD2.

To get an idea about the quality of the proposed broadband shortcut to AOD500, we applied Gueymard's (1998) parameterization, based on his known SMARTS2 model. Apparently due to a wider than traditional field of view (FOV = 10°) of the Tõravere actinometer AT50, values of the broadband direct beam in our database are slightly overestimated in cases of larger aerosol turbidity. This explains slightly under-

estimated AOD500 as predicted by Gueymard's parameterization. Despite this systematic difference, there was a very high consistency (coherence) between both predicted results, expressed by the coefficient of determination, $R^2 = 0.994$.

2. A THREE-LAYER STRUCTURE OF COLUMN BROADBAND TRANSMITTANCE

Spectral content of the direct solar beam reaching the Earth's surface is not equal during a day. Broadband characteristics, therefore, depend on solar elevation even in the case of stationary and azimuthally homogeneous atmosphere, causing the Forbes effect – virtual diurnal variation in atmospheric broadband optical characteristics (Ohvriil et al., 1999).

For this effect, even though spectral optical depth and related spectral optical parameters (transmittance, the Bouguer coefficient, etc.), are independent of optical mass m , their broadband counterparts are not. Although there are no good solutions for strict transformation of column broadband optical parameters from one solar elevation to another, multiannual pyrheliometric time series, recorded at various stations, mainly on the territory of the former USSR, have stimulated creation of corresponding semi-empirical methods. Historically, a destination optical mass, $m = 1$, was initially chosen (Kalitin, 1938). However, for control measurements the case where the Sun is at the zenith, is not available at most radiometric stations. The next integer number, $m = 2$ (solar elevation angle about 30°), was further preferred as a standard one in interpretation of pyrheliometric observations. A set of simple formulas links different broadband optical parameters like the Bouguer coefficient of transparency, transmittance, optical depth, the Linke turbidity factor (Ohvriil et al., 2009). Concerning aerosol optics, the same reference air mass is also recommended (Gueymard and Kambezidis, 1997).

We further limit the structure of extinction of the broadband direct solar beam by three processes or substances:

- (a) an ideal or clean and dry atmosphere (CDA), which includes Rayleigh scattering, absorption by ozone (O₃), and nitrogen dioxide (NO₂);
- (b) integrated column water vapour or precipitable water, W ;
- (c) atmospheric aerosol particles.

Denoting their transmittances by $\tau_{\text{CDA},m}$, $\tau_{W,m}$, and $\tau_{\text{aer},m}$, respectively, it is of considerable computational convenience to express the incident broadband beam irradiance at normal surface, “beam irradiance”, S_m , as a direct product of individual beam transmittances which is equal to a presumption of three successive extinction layers (Gueymard, 1998):

$$S_m = S_0 \tau_{\text{CDA},m} \tau_{W,m} \tau_{\text{aer},m}, \quad (1)$$

where S_0 is the extraterrestrial broadband irradiance at the actual Sun–Earth distance, its average value, the “solar constant”, is 1.367 kW m^{-2} (Lenoble, 1993).

On the other hand, using broadband total transmittance, τ_m , and the Bouguer coefficient of transparency, p_m (Kondratyev, 1969):

$$p_m = \left(\frac{S_m}{S_0} \right)^{\frac{1}{m}}, \quad (2)$$

we can also express S_m as

$$S_m = S_0 \tau_m = S_0 p_m^m, \quad (3)$$

which gives for broadband aerosol transmittance

$$\tau_{\text{aer},m} = \frac{p_m^m}{\tau_{\text{CDA},m} \tau_{W,m}}. \quad (4)$$

By similarity with Bouguer formula which, strictly speaking, is valid only for a monochromatic beam, the following equation defines broadband aerosol optical depth, BAOD_m , which we denote in formulas by $\delta_{\text{aer},m}$ (Gueymard, 1998):

$$\tau_{\text{aer},m} = \exp(-m \delta_{\text{aer},m}). \quad (5)$$

Combining this definition with (4), we obtain for BAOD_m :

$$\delta_{\text{aer},m} = -\frac{1}{m} \ln \tau_{\text{aer},m} = -\frac{1}{m} \ln \frac{p_m^m}{\tau_{\text{CDA},m} \tau_{W,m}}, \quad (6)$$

$$\delta_{\text{aer},m} = -\ln p_m + \frac{1}{m} \ln \tau_{\text{CDA},m} + \frac{1}{m} \ln \delta_{W,m}. \quad (7)$$

BAOD_m is equal to the Unsworth–Monteith turbidity coefficient (Unsworth and Monteith, 1972; Gueymard, 1998). This parameter can be used to estimate aerosol contribution in attenuation of the broadband direct beam, in addition to a clean-wet atmosphere, consisting of CDA and water vapour only (Kambezidis et al., 1998).

We now continue with $m = 2$ and have for BAOD_2 :

$$\begin{aligned} \text{BAOD}_2 = \delta_{\text{aer},2} &= -\frac{1}{2} \ln \tau_2 + \frac{1}{2} \ln \tau_{\text{CDA},2} + \frac{1}{2} \ln \tau_{W,2} \\ &= -\ln p_2 + \ln p_{\text{CDA},2} + \frac{1}{2} \ln \tau_{W,2}. \end{aligned} \quad (8)$$

Calculation of BAOD_2 is now reduced to availability of three broadband quantities: (a) τ_2 or p_2 as results of broadband direct beam observations of S_m and following recalculations of τ_m to τ_2 or p_2 , in

order to go from optional m to a fixed one, $m = 2$; (b) $\tau_{\text{CDA},2}$ or $p_{\text{CDA},2}$ which should be calculated from models of ideal atmosphere, CDA; (c) $\tau_{W,2}$ which first needs estimation of column precipitable water at zenith direction, W , and, as a second step, calculation of transmittance of column water vapour for the entire slope column, $m = 2$.

There are two methods to obtain the Bouguer coefficient of transparency p_2 from S_m observations, which both give close results (Ohvriil et al., 1999). In Russia and Ukraine, p_2 is calculated directly from the observed broadband direct beam S_m , using the Evnevich–Savikovskij formula (Evnevich and Savikovskij, 1989):

$$p_2 = \left(\frac{S_m d^2}{1.367} \right)^{\frac{\sin h + 0.205}{1.41}}, \quad (9)$$

where d is the actual Earth–Sun distance in astronomical units. In Estonian actinometric practice the Bouguer coefficient of transparency, p_m , is first calculated using Eq. (2). As a second step, p_2 is recalculated from p_m using the formula that has been founded by Mürk and Ohvriil (Myurk and Ohvriil, 1990; Ohvriil et al., 1999):

$$p_2 = p_m \left(\frac{2}{m} \right)^{\frac{\log p_m + 0.009}{\log m - 1.848}}. \quad (10)$$

Broadband coefficients of transparency, $\tau_{\text{CDA},2}$, of a CDA, depend, besides molecular (Rayleigh) scattering, on absorption by trace gases, mainly by O_3 and NO_2 . For that, column amounts of trace gases should be first estimated.

3. EVALUATION OF COLUMN NO_2 AMOUNTS

Vertical NO_2 profiles as described by standard atmospheres usually refer to very clean areas without intensive combustion processes and therefore the column amounts are low. The 1976 U.S. Standard Atmosphere – USSA 1976 (Thomas and Stamnes, 2002) gives for the tropospheric (0–11 km) NO_2 column amount only $0.386 \times 10^{15} \text{ molecules cm}^{-2}$. Normalizing this result with the Loschmidt constant ($2.69 \times 10^{19} \text{ molecules cm}^{-3}$, 0°C , 1 atm), we obtain for the tropospheric NO_2 layer column thickness $1.4 \times 10^{-5} \text{ cm}$, which we denote, following Gueymard’s (1998) nomenclature, as 0.014 matm cm ($\equiv 0.014 \text{ DU}$). However, this tropospheric NO_2 content seems to be considerably underestimated compared to present-day European values.

Since the 1980s, the global mapping of column NO_2 has been possible with the help of satellites. Tropospheric NO_2 geography, with special focus on

Central and Northern Europe and the Baltic Sea Region, is given by Ionov (2010). His review, for 2004–2009, shows low tropospheric NO₂ for Estonia, $(0.8–1) \times 10^{15}$ molecules cm⁻², or 0.03–0.037 matm cm. High tropospheric NO₂ values were found over St. Petersburg (up to 9×10^{15} molecules cm⁻² or 0.335 matm cm), and even higher values over Belgium, Netherlands, Germany, and Moscow (up to 18×10^{15} molecules cm⁻² or 0.669 matm cm).

An extended review on stratospheric NO₂ global distribution is given by Dirksen et al. (2011). For latitudes 25°–65° the NO₂ annual mean is about 3.2×10^{15} molecules cm⁻² or 0.12 matm cm. The thinnest stratospheric NO₂ layer is on the equator, 0.5×10^{15} molecules cm⁻² or 0.019 matm cm. The amplitude of the seasonal cycle increases with latitude, with the largest stratospheric NO₂ column over the South Pole in summer, 6×10^{15} molecules cm⁻² or 0.223 matm cm.

4. BROADBAND TRANSMITTANCES FOR SOME CDAs

In order to get a picture about variability of column transparency of ideal atmospheres with different O₃ and NO₂ contents, we made numerous runs of Gueymard's (1998) parameterization. Table 1 shows three typical of them. Row 1 corresponds to very low concentrations: 150 DU (0.15 atm cm) for O₃ and only 88 pptv (10^{-12}) for total NO₂ column amount. The ozone content of 350 DU (0.35 atm cm), in row 2, represents an annual mean for Estonia (Okulov, 2003; Okulov and Ohvriil, 2010; Veismann and Eerme, 2011). The NO₂ amounts are also typical of this region.

The table exhibits a relatively small sensibility of transparency and transmittance of different CDAs (the last three columns) to changes in column concentrations of trace gases. Considering now that the relative error of the observed (by an actinometer) broadband direct beam is $\pm 4\%$ which leads to $\pm 2\%$ errors in coefficients p_2 , we can assume that $\ln p_{\text{CDA},2} \approx -0.1$ and rewrite (8) in a simpler form:

$$\text{BAOD2} = -\ln p_2 - 0.1 + \frac{1}{2} \ln \tau_{w,2}. \quad (11)$$

5. BROADBAND TRANSMITTANCE OF COLUMN WATER VAPOUR

In order to calculate the ability of solar radiation to pass the atmospheric water vapour, the amount of total column water vapour, W , should first be estimated. The number of measurement techniques for W observations has increased considerably since the 1990s and now includes ground-based and space-borne optical soundings, microwave radiometry, as well as propagation delay estimation using ground-based GPS data. In most countries, however, the classic balloon-borne radiosounding remains the main routine method for W monitoring (Jakobson et al., 2009), but the network of radiosonde stations is sparse and sondes are launched only 1–2 times per day. Therefore, especially for solar radiation and aerosol studies, correlation between W and surface meteorological parameters (mainly surface temperature and pressure of water vapour) is used. A short historical review of approximate calculations of W is listed by Okulov et al. (2002). For the Baltic region Jakobson et al. (2005) expressed seasonal means of W as linear functions of the geographical latitude degree.

Suppose that the amount of W is already known. To investigate how W affects broadband transmittance through a hypothetical atmosphere consisting of water vapour only, we have to use some kind of radiative transfer model. However, there are two major problems: (a) the complexity of the extraterrestrial solar spectrum and (b) the peculiarity of the water molecule, leading to an extremely complicated vibration-rotation absorption spectrum (Maurellis and Tennyson, 2003).

Nevertheless, during the last decades progress has been made in models calculating the water vapour attenuation of the broadband solar beam, leading to larger values of absorption. This statement follows, for example, from comparing parameterizations proposed by Zvereva (1968) and Gueymard (1995, 1998).

For the calculation of extinction of broadband solar beam irradiance, we recommend the parameterization developed by Gueymard (1995, 1998), based on his SMARTS2 model. He used a solar spectrum of 1881 wavelengths, at 1-nm intervals within the most

Table 1. Results of Gueymard's (1998) parameterization runs to obtain broadband column transparencies ($p_{\text{CDA},2}$ and logarithm of it) and transmittances ($\tau_{\text{CDA},2}$) of ideal atmospheres with different O₃ and NO₂ contents

No.	O ₃ , atm cm	NO ₂				$p_{\text{CDA},2}$	$\ln p_{\text{CDA},2}$	$\tau_{\text{CDA},2}$
		tropos, atm cm	stratos, atm cm	tro+stra, atm cm	tro+stra, pptv			
1	0.15	0.000 03	0.000 04	0.000 07	88	0.9081	-0.0964	0.8246
2	0.35	0.000 04	0.000 120	0.000 160	200	0.9042	-0.1007	0.8176
3	0.60	0.001 00	0.000 200	0.001 200	1501	0.8998	-0.1056	0.8096

important part of the spectrum (280–1700 nm). Although the method consists of 20 formulas, Ohvril et al. (2005) demonstrated that in a particular case, for atmospheric optical mass $m = 2$, the transmittance of water vapour can be expressed by a single formula:

$$\tau_{W,2} = 1 - 0.137W^{0.32}, \quad (12)$$

where W (cm) is precipitable water in the zenith direction.

Plots of transmittances $\tau_{W,2}$, calculated according to Zvereva (1968), Gueymard (1998), and Ohvril et al. (2005), are given in Fig. 1.

Two results are evident: (a) approximation (12) provides an excellent agreement with Gueymard’s complicated parameterization – visually the two lower curves in Fig. 1 are difficult to distinguish from each other and (b) Gueymard’s method gives considerably stronger attenuation of direct solar beam irradiance than the model by Zvereva 30 years before.

Broadband optical depths of water vapour:

$$\delta_{W,2} = -\frac{1}{2} \ln \tau_{W,2}$$

are plotted in Fig. 2. As expected, Gueymard’s parameterization, for $m = 2$, can be successfully replaced by (12), but Zvereva’s model considerably underestimates the optical depth of column water vapour.

The curves of Gueymard and Ohvril et al., plotted in Figs 1 and 2, allow quick estimation of broadband transmittance and broadband optical depth of water vapour, at $m = 2$, for any zenith precipitable water W . For example, a planetary mean column humidity, $W = 2.5$ cm (Peixoto, 1992) corresponds to transmittance 0.82 and optical depth 0.10. Typical summer precipitable water in the Baltic area, 2.0 cm, gives a transmittance of 0.83, and an optical depth of 0.094. During winter, at lower column humidity, transmittance and optical depth are more sensible to W changes (see

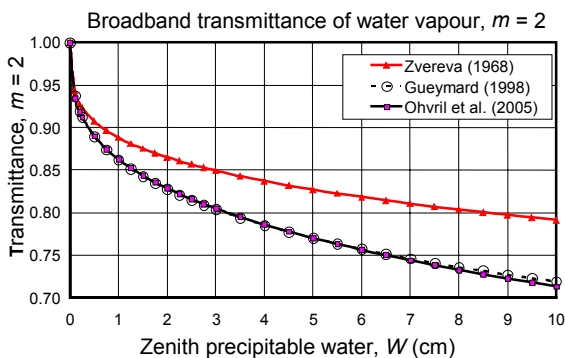


Fig. 1. Broadband transmittances of water vapour for optical mass $m = 2$ (solar elevation $\approx 30^\circ$) as functions of precipitable water in the zenith direction, W .

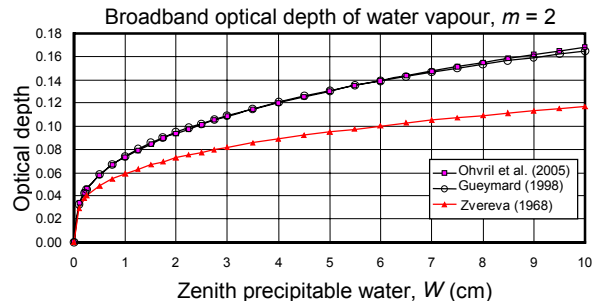


Fig. 2. Broadband optical depths of water vapour for optical mass $m = 2$ (solar elevation $\approx 30^\circ$) as functions of precipitable water in the zenith direction, W .

Figs 1 and 2), but the average diurnal peak-to-peak (PtP) changes in W are usually low, e.g. in the Baltic region, PtP = 0.64 mm for summer and only 0.2 mm for winter. Of course, W can show fast variations, reaching up to 5 mm h^{-1} during several hours, but exclusively during changes in the synoptic situation and substitution of airmasses above the location of observation (Jakobson et al., 2009). We should not worry about these transitional cases, because, as a rule, cloudiness restricts observations of direct solar beam during synoptic changes.

Substitution of (12) into (11) gives the final equation for BAOD2:

$$\text{BAOD2} = -\ln p_2 - 0.1 + \frac{1}{2} \ln[1 - 0.137W^{0.32}], \quad (13)$$

where zenith W is in centimetres. This formula is one of the main results of the given work. Below it will be used for transition from BAOD2 to AOD500.

Figure 3 gives a visual review about limits of the extent of BAOD2 as a function of p_2 and W . As input we have used five values for precipitable water. The

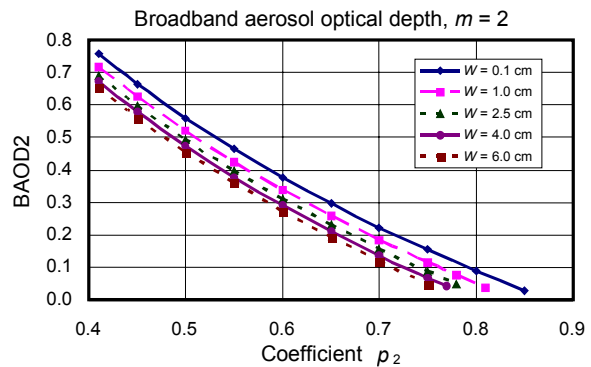


Fig. 3. Broadband aerosol optical depth as plotted against the broadband column transparency coefficient. Calculations are implemented for $m = 2$ and a set of values of zenith precipitable water, from $W = 0.1$ to 6.0 cm.

lowest one, $W = 0.1$ cm, corresponds to a cold winter atmosphere, $W = 1.0$ cm is typical in Estonia in April and October (Okulov, 2003; Okulov and Ohvril, 2010). As mentioned, $W = 2.5$ cm is a planetary mean. During hot and sultry summer days in Estonia, a value $W = 4.0$ cm has been reached, and finally, $W = 6.0$ cm corresponds to a tropical atmosphere. The figure allows a rough evaluation of the change in BAOD2 due to a change in W , for a given coefficient of transparency, p_2 . Considering small PtP changes in diurnal evolution of W , BAOD2 has a low diurnal variability due to W .

A practical note should be made. Obviously, a condition

$$\text{BAOD2} \geq 0 \quad (14)$$

should be followed. However, sometimes calculations according to (13) give negative results. It usually happens because of overestimation of W using approximate methods. For that, during inspection of radiation and column humidity databases, a control should be made to remove incompatible pairs of p_2 and W . Apparently, in the absence of aerosol attenuation, $\tau_{\text{aer},m} = 1$, and it follows from (4) that condition (14) is equal to

$$p_2 \leq p_{2,\text{max}} = [\tau_{\text{CDA},2} \tau_{W,2}]^{0.5} \approx [0.817 - 0.112W^{0.32}]^{0.5}, \quad (15)$$

where $p_{2,\text{max}}$ is, for given W , the maximal possible value of p_2 in a wet and clean atmosphere (Fig. 4). Insertion of aerosol particles into a wet and clean atmosphere would diminish values of column transparency, p_2 .

For a typical precipitable water summer value in Estonia, $W = 2$ cm, a maximal coefficient of column transparency is: $p_{2,\text{max}} \approx 0.82$, for the highest Estonian value $W = 4$ cm, calculation gives 0.80.

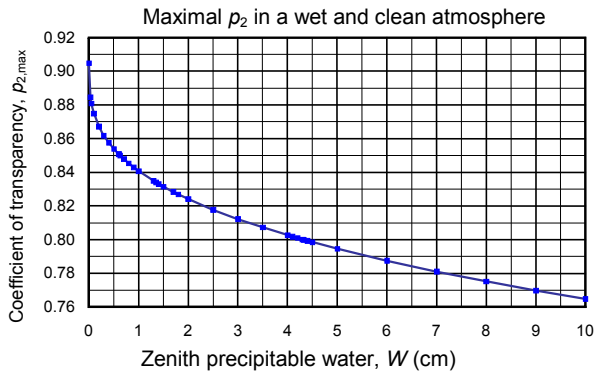


Fig. 4. Maximal possible broadband Bouguer coefficients of transparency, $p_{2,\text{max}}$, for a clean and wet atmosphere.

6. COMPARING SPECTRAL AND BROADBAND OPTICAL DEPTHS

Routine measurements of broadband solar direct irradiance started in Estonia already in 1931. In addition to a wide set of broadband observations during several decades, regular measurements of spectral solar direct irradiance started at Tõravere in June 2002. An autonomous AERONET sunphotometer, Cimel CE 318-1, generously provided by B. Holben's team from the NASA Goddard Space Flight Center, is used. Simultaneous registration of both spectral and broadband irradiances enables comparison of spectral and broadband parameters of transparency or turbidity and development of approximate methods for evaluation of $\text{AOD}\lambda$ using only broadband parameters and integrated column water vapour.

In this work we have used 19 592 complex observations from all seasons during 2002–2009, when, within 10 min, both spectral and broadband direct irradiances were measured. Precipitable water (in mm) was calculated according to an approximation

$$W(e_0) = 1.48e_0 + 0.40, \quad (16)$$

where e_0 (mb) is the 12 UTC ground water vapour pressure. This parameterization was developed according to clear sky radio-soundings in Tallinn (Okulov et al., 2002). Note that unlike W , ground water vapour pressure, e_0 , has a remarkable diurnal cycle. For that, in approximations like (16), the e_0 should correspond to a fixed time, e.g. to 12 GMT. This condition, obviously, leaves the estimated column humidity unchangeable during a day.

Figure 5 compares column humidity, $W(e_0)$, estimated by surface water vapour pressure values with $W(\text{AERONET})$ which are considered as reference values. As an average, prediction overestimates the

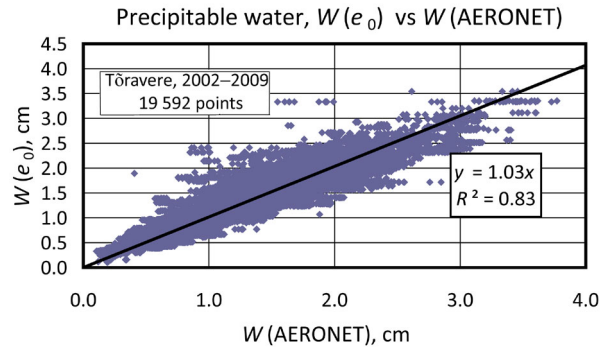


Fig. 5. Precipitable water $W(e_0)$, estimated using ground water vapour pressure, is plotted against reference precipitable water $W(\text{AERONET})$, calculated from solar photometry (Tõravere, 2002–2009, 19 592 points).

reference only by 3%, but the coefficient of determination, $R^2 = 0.83$ only, indicates a substantial scatter of $W(e_0)$ around $W(\text{AERONET})$.

In cases of relatively dry winter air ($W < 0.5$ cm) prediction of W by (16) has a root mean square deviation (RMSD) equal to 0.135 cm (Table 2, the 1st column). Compared to the mean value of this particular range, $W = 0.25$ mm, the deviation is 54%.

For higher W amounts the relative RMSD is lower, reaching a final level of $\text{RMSD} \approx 11\text{--}12\%$ for $W(\text{AERONET}) > 2$ cm. Note that uncertainty in $W(\text{AERONET})$ is typically less than 12% (Holben et al., 1998).

In Figure 6 two sets of broadband optical depth, BAOD2, calculated by (13) are compared. For both sets, the same input of observed column transparency, p_2 , is used but with two different values for precipitable water, $W(\text{AERONET})$ and $W(e_0)$, respectively. Both BAOD2s are strongly correlated, $R^2 = 0.993$, having an excellent linear relationship, $y = 0.997x$. This result confirms that BAOD2 is not sensitive to estimations of precipitable water.

The relationship between the spectral AOD and its broadband counterpart, BAOD2, is presented in Fig. 7.

Table 2. Root mean square deviations (RMSD) of W prediction for different W ranges

	$W(\text{AERONET})$ range, cm						
	0–0.5	0.5–1.0	1.0–1.5	1.5–2.0	2.0–2.5	2.5–3.0	3.0–4.0
Observations, % of 19 592	9.6	25.6	27.0	22.6	11.6	2.7	0.9
RMSD, mm	0.135	0.239	0.287	0.293	0.271	0.300	0.368
Relative RMSD, %	54	32	23	17	12	11	11

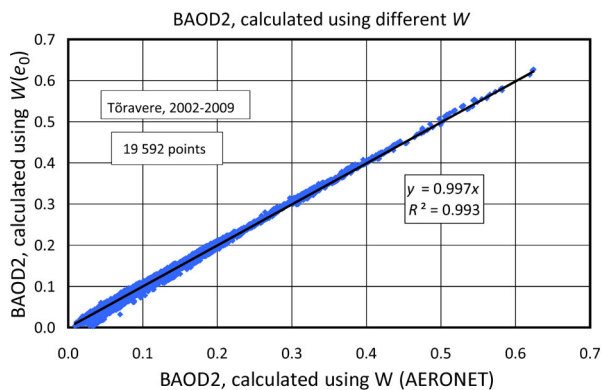


Fig. 6. Broadband aerosol optical depth (BAOD2, $m = 2$) calculated using column humidity $W(e_0)$, estimated by surface water vapour pressure, is plotted against the BAOD2 estimated by $W(\text{AERONET})$ (Tõravere, 2002–2009, 19 592 points).

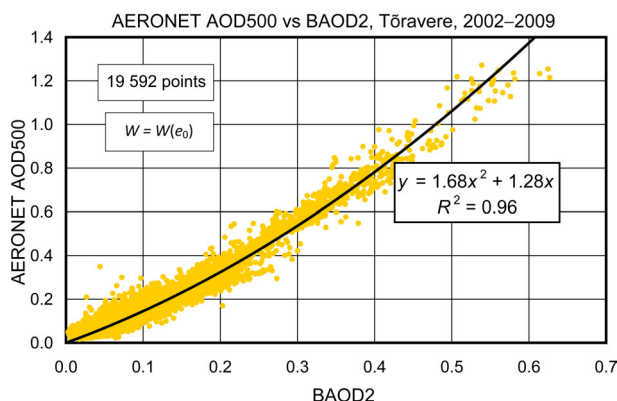


Fig. 7. AOD500 as observed by AERONET at Tõravere, Estonia, plotted against the broadband aerosol optical depth, BAOD2, for optical mass $m = 2$ (2002–2009, 19 592 points).

Here a large set (the same 19 592 joint observations from 2002–2009) of AOD500, observed by the AERONET sunphotometer (Level 2, Version 2) at Tõravere, are plotted against the BAOD2 calculated by (13).

Recall that the results plotted in Fig. 7 were developed for the given location but without any presumptions about the properties of aerosol particles in the column (the Ångström exponent, size distribution, absorption coefficient, etc.). The two optical depth parameters AOD500 and BAOD2 are strongly correlated ($R^2 = 0.96$) through the following second-degree polynomial:

$$\text{AOD500} = 1.7(\text{BAOD2})^2 + 1.3(\text{BAOD2}), \quad (17)$$

where BAOD2 is calculated by (13) using observed coefficients of column broadband transparency, p_2 , and column humidity, $W(e_0)$, is estimated by a simple model (16). As expected, replacement of $W(e_0)$ by $W(\text{AERONET})$ caused only negligible changes in Fig. 7 (a respective figure with this test is not presented).

In Fig. 8, AOD500, predicted by (17), using BAOD2 as a function of p_2 and $W(e_0)$, is compared to the reference AOD500 as observed by AERONET at Tõravere. Here 81.8% of points belong to the range $\text{AOD500}(\text{AERONET}) < 0.2$ where the RMSD between predicted and reference values is 0.022. The last number apparently represents uncertainty of this quite rough broadband approach to predict AOD500 for a quite typical turbidity range at a particular geographical location – Tõravere. For comparison, the instrumental uncertainty in $\text{AOD500}(\text{AERONET})$ is 0.01 (Holben et al., 1998). The RMSD of prediction increases with increasing AOD500, and reaches 0.106 in very turbid cases when $\text{AOD500} = 1.0\text{--}1.3$ (Table 3).

Relative RMSD, with regard to the middle value of the first range, $\text{AOD500} = 0.1$, is 22% and less than 12% for higher turbidities. This accuracy is not bad,

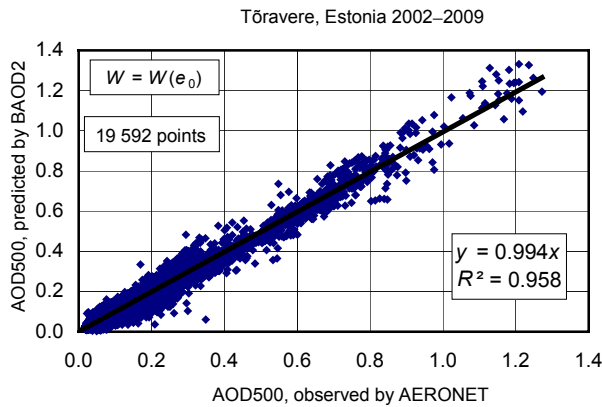


Fig. 8. AOD500 as predicted by broadband aerosol optical depth, BAOD2 at $m = 2$, plotted against AOD500 as derived from the AERONET Tõravere observations from 2002–2009 (19 592 points).

Table 3. RMSD of AOD500 prediction at different turbidity ranges (Tõravere)

	AOD500 range					
	0.0–0.2	0.2–0.4	0.4–0.6	0.6–0.8	0.8–1.0	1.0–1.3
Observations, % of 19 592	81.8	13.8	2.3	1.5	0.4	0.2
RMSD, mm	0.022	0.035	0.042	0.047	0.081	0.106
Relative RMSD, %	22	12	9	7	9	9

reminding us again that in creating this broadband approach, no presumptions were made about season, meteorological situation, microphysical parameters of aerosol particles, etc. For the entire observed range of optical depth, covering the $AOD500 = 0–1.3$, there is an excellent linear relationship ($y = 0.994x$) and close correlation ($R^2 = 0.958$) between predicted and reference AERONET values.

Can we expect for a better prediction of AOD500, using a more advanced complicated broadband approach? Apparently, one of the best broadband parameterizations, until now, is based on the SMARTS2 model which was developed by Gueymard (1995, 1998). It allows transition from broadband solar irradiance, S , to AOD1000 (the model’s basic wavelength, $\lambda = 1000$ nm). As a parametric input, the model uses precipitable water W , columnar O_3 and NO_2 contents, and a fixed Ångström exponent, $\alpha = 1.3$. Using Ångström’s classic formula, AOD1000, by multiplication to $(1000/500)^{1.3} = 2.46$, is easily recalculated to AOD500.

Running Gueymard’s model, we inserted from observations: broadband solar irradiance, S_2 (optical mass $m = 2$, average Sun–Earth distance) and zenith precipitable water, W . We assumed columnar O_3 and NO_2 contents as all-year climatological averages.

Figure 9 shows AOD500(Gueymard) as predicted by Gueymard’s model, against AOD500(AERONET) as observed at Tõravere. For larger turbidities, $AOD500 > 0.4$, the figure shows increasing underestimation of AOD500 by Gueymard’s model. This discrepancy can mainly be explained by a peculiarity of Savinov–Yanishevsky thermoelectric actinometers (operational pyr heliometers) AT50, used for observations of broadband direct beam at Tõravere. This cheap but reliable instrument has a 10° field of view (FOV). For comparison, the Eppley pyr heliometer’s FOV is only 5.7° . In the case of turbid atmosphere, the bigger FOV leads to a “parasitic” circumsolar radiation, which increases the observed direct solar beam, S , and creates an illusion about better transparency and lower turbidity. Inserting the increased S into Gueymard’s model, one apparently obtains slightly lower AOD values.

Disagreement between the AOD500, predicted by BAOD2, and by Gueymard’s model, is clearly seen in Fig. 10 where the same inputs for both models are used. The AOD500, derived from BAOD2, predicts higher values than AOD500(Gueymard), and better compensates the circumsolar radiation in the case of larger turbidities. Of course, following the suggestion proposed by Carlund et al. (2003), it is possible to derive respective correction for Gueymard’s model in order to increase predicted AOD500 values in the case of pyr heliometers with a larger FOV.

What is remarkable in Fig. 10 is a close convergence of points around a parabolic regression line,

$$y = 0.383x^2 + 0.888x, \quad (18)$$

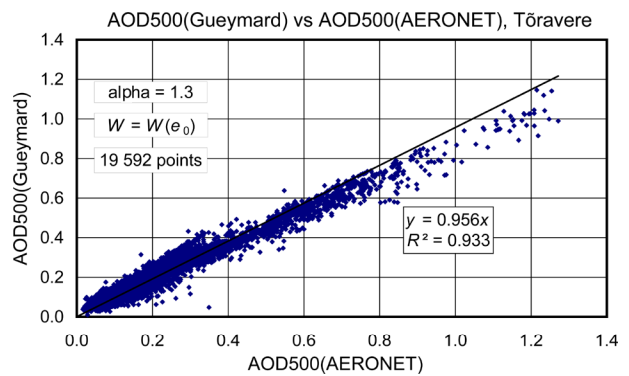


Fig. 9. AOD500(Gueymard) as predicted by Gueymard’s model, plotted against AOD500(AERONET) as derived from the AERONET Tõravere observations (19 592 points from 2002–2009).

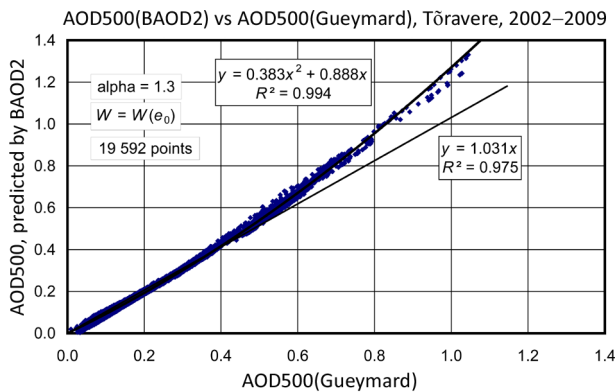


Fig. 10. AOD500 as predicted by BAOD2, plotted against AOD500(Gueymard) using the same inputs of the broadband direct beam and predicted precipitable water from Tõravere observations during 2002–2009 (19 592 points).

where $x = \text{AOD500(Gueymard)}$. A very high coefficient of determination, $R^2 = 0.994$, indicates, despite systematic discrepancy, a dense coherence of AOD500, predicted by our rough shortcut model and by an advanced Gueymard's model, respectively.

7. TEST AGAINST AERONET OBSERVATIONS

Performance of the proposed model, expressed by Eq. (17) and based on data from Tõravere, 2002–2009, was first tested against fresh reference AOD500 AERONET–Tõravere observations from 2010. Single values and daily averages were compared (Fig. 11).

Figure 11 shows a close consistency between predicted and reference data. For single values the determination coefficient was $R^2 \approx 0.97$, and for daily

means even higher, $R^2 \approx 0.98$. The slope of the regression, $y = 1.08x$, seems somewhat high. However, the slope varies between 0.93 and 1.08 in prediction for single years during 2002–2009. Apparently, uncertainty for the slope is about 8%.

8. TESTS AGAINST TERRAMODIS AND AQUAMODIS OBSERVATIONS

Both Terra- and AquaMODIS allow download of daily means of AOD550 and Ångström exponents for 1×1 deg pixels on the underlying surface. Using the Ångström formula, AOD550 can be recalculated to AOD500. In this work we considered Tõravere in the centre of the 1×1 deg area. During 2010, there were 94 days when data from all three AOD instruments as well as from a broadband actinometer were available. Results of AOD500 comparisons are plotted in four panels of Fig. 12.

The left panels represent tests of AquaMODIS and TerraMODIS against daily means of AERONET as a reference instrument. Although the uncertainty for the slope is about 6% only, the consistency of data in both cases is low, $R^2 = 0.775$ and 0.702, respectively.

In the right panels the AOD500 daily means from BAOD are tested against TerraMODIS and AquaMODIS, respectively. As expected, the uncertainty for the slope is greater, about 10%, and the consistency is lower than comparing against AERONET data, $R^2 = 0.749$ and 0.683, respectively. But, what is special in all panels of Fig. 12, is a possibility of getting negative AOD values by both satellites. Apparently, this kind of mistake happens due to overestimation of column precipitable water, W .

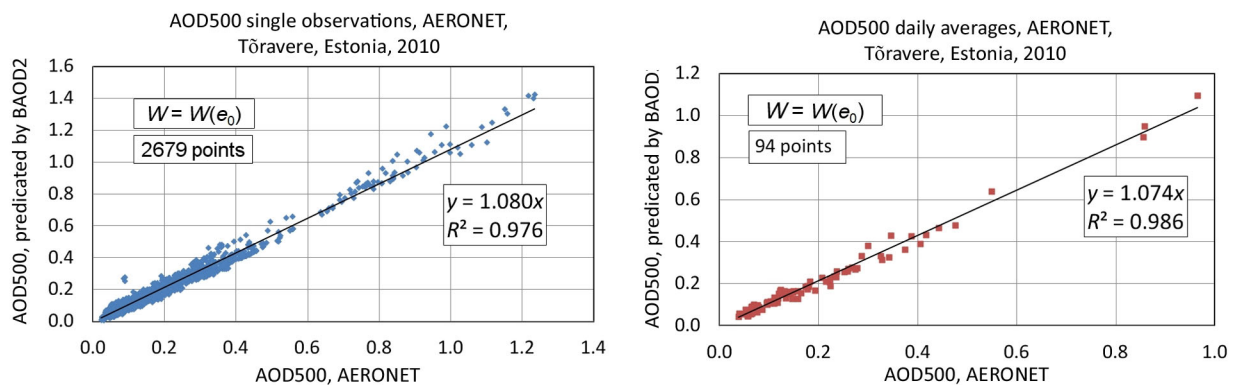


Fig. 11. AOD500 as predicted by broadband aerosol optical depth, BAOD2 at $m = 2$, plotted against AOD500 from the AERONET Tõravere 2010 observations. The left panel represents 2679 single observations, the right panel 94 daily means.

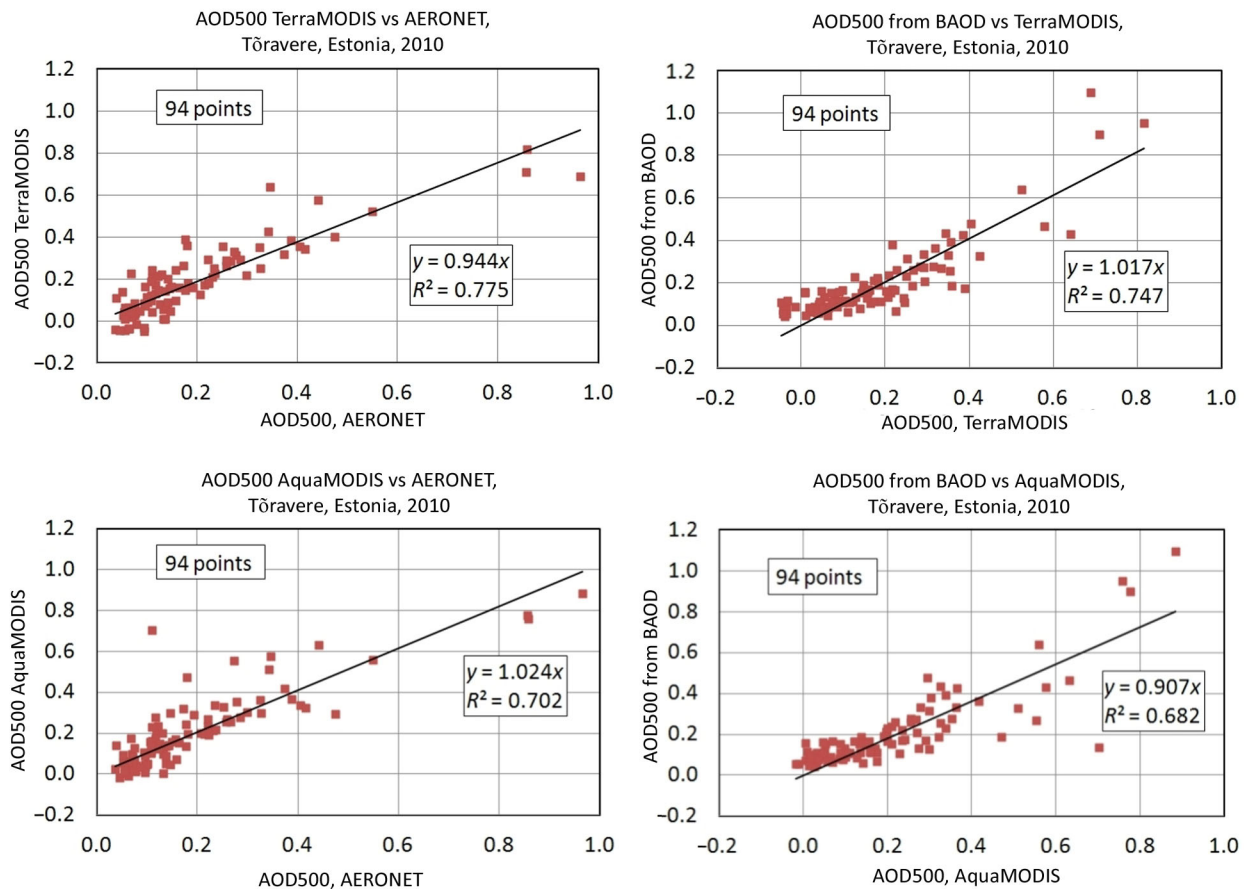


Fig. 12. The left panels: AOD500 daily means from the MODIS satellites, plotted against the reference, AERONET Tõravere observations. The right panels: AOD500 daily means as predicted by broadband aerosol optical depth, BAOD2, plotted against AOD500 observed by the MODIS satellites. Note that in several occasions the satellite AOD500 values are negative.

9. CONCLUSIONS AND DISCUSSION

The following conclusions can be drawn from this study.

- (A) For prediction of AOD500, a simple “short-cut” broadband model is proposed. As an input, the model uses two quantities: (a) column broadband Bouguer coefficient of transparency, p_2 , which corresponds to optical mass, $m = 2$; and (b) column precipitable water, W . According to the input, a broadband aerosol optical depth, BAOD2, for the same solar elevation is calculated. Transition from BAOD2 to AOD500 is implemented using an experimental parabolic relationship (17). The “short-cut” model is based on a large database, 19 592 joint broadband (provided by the EMHI – Estonian Meteorological and Hydrological Institute), and spectral (provided by the AERONET) observations during all seasons of 2002–2009. In the database, 81.8% of observations corresponded to aerosol optical depth, AOD500 < 0.2. In this range of

aerosol turbidity, the RMSD of prediction was 0.022. For comparison, the instrumental uncertainty in AOD500(AERONET) is 0.01 (Holben et al., 1998). Absolute deviations of prediction increased towards increase in AOD500 and were 0.035 for the next range of aerosol turbidity, 0.2–0.4 (13.8% of observations). For very turbid cases, when AOD500 = 1.0–1.3, the RMSD reached 0.11.

- (B) Performance of the model was tested using fresh data – 2679 joint, broadband (provided by the EMHI) and spectral (AERONET) single observations during all seasons of 2010 at Tõravere. In terms of regression, the uncertainty in prediction (against AERONET reference values) was about 8%. The consistency between predictions and the reference values was surprisingly good, $R^2 = 0.976$ for single observations and $R^2 = 0.986$ for daily means.

The model was also verified using named 94 daily average values during 2010, when the AOD data from TerraMODIS and AquaMODIS were

available besides the AERONET and broadband actinometer observations. The values of AOD500 obtained by all four methods were roughly comparable but consistency of satellite data against the AERONET and broadband model was low. It should be noted that in several occasions the AOD from satellites is negative, apparently due to overestimation of column precipitable water, W .

- (C) One of the inputs of the model, column precipitable water, W , was calculated using its correlation with surface water vapour pressure, e_0 . It appeared that neither BAOD2 nor AOD500 was sensible to the W input. Replacement by $W(e_0)$ to a more correct W (AERONET) did not improve predictions.
- (D) For an additional examination of our AOD500 predictions, Gueymard's broadband model (1998) was used. Our predictions systematically exceeded Gueymard's ones, a linear regression, $y = 1.031x$, was applicable for $\text{AOD500} < 0.5$. For larger turbidities difference between predictions started to increase. Apparently, this discrepancy is not a shortcoming of Gueymard's model but due to a large (10°) field of view (FOV) of the AT50 actinometer used at Tõravere for observations of the broadband direct solar beam. A larger FOV than that of conventional pyrhemometers (5.7°) enables more circumsolar radiation enter an instrument, which increases the observed direct solar beam and creates an impression about better transparency and lower turbidity.

When problems with circumsolar radiation which can be corrected with adjusting constants were ignored, both broadband models (our model and Gueymard's parameterization) demonstrated a surprising consistence of prediction between each other (Fig. 10), with a very high coefficient of parabolic regression, $R^2 = 0.994$.

The listed results lead to a speculation about the ability of a broadband approach to predict spectral AOD λ . Climatology of AOD λ , as well as of any other aerosol optical parameter, emphasizes its high variability (Olmo et al., 2001; Smirnov et al., 2002; Aaltonen et al., 2006; Toledano et al., 2007). Apparently, this variability can be only in part observed and predicted with broadband methods. Perhaps, using additional information on the column aerosol content (like the origin, seasonality and diurnal trend of particles, their size distribution, etc.), particular models can be created and the quality of AOD λ prediction improved.

On the other hand, the introduced simple broadband "shortcut" can be recommended for estimation of column AOD500 using data on broadband direct irradiance archived in the past, and explain climatological trends related to volcanic activity, anthropogenic pollution, etc.

In radiometric stations, where spectral and broadband solar direct beams are currently observed, the method can also be used for quality control of automated AOD500 observations.

Obviously, for different geographical locations, adjusting constants in formulas (16) and (17) are not identical with the given ones, developed for Tõravere, Estonia.

ACKNOWLEDGEMENTS

This work was funded by the Estonian Research Council (grant 7347 and project SF0180038s08) and the European Regional Development Fund, project "Estonian Radiation Climate". We thank the Estonian Meteorological Institute and the AERONET team for performing observations at Tõravere and making available their unique databases.

REFERENCES

- Aaltonen, V., Lihavainen, H., Kerminen, V.-M., Komppula, M., Hatakka, J., Eneroth, K., Kulmala, M., and Viisanen, Y. 2006. Measurements of optical properties of atmospheric aerosols in Northern Finland. *Atmos. Chem. Phys.*, **6**, 1155–1164.
- Carlund, T., Landelius, T., and Josefsson, W. 2003. Comparison and uncertainty of aerosol optical depth estimates derived from spectral and broadband measurements. *JAM*, **42**, 1598–1610.
- Dirksen, R. J., Boersma, K. F., Eskes, H. J., Ionov, D. V., Bucsela, E. J., Levelt, P. F., and Kelder, H. M. 2011. Evaluation of stratospheric NO₂ retrieved from the Ozone Monitoring Instrument: intercomparison, diurnal cycle, and trending. *J. Geophys. Res.*, **116**, D08305.
- Evnevich, T. V. and Savikovskij, I. A. 1989. Calculation of direct solar radiation and coefficient of atmospheric transparency. *Soviet Meteorol. Hydrol.*, **5**, 92–95.
- Gueymard, C. 1995. *SMARTS2, a Simple Model of the Atmospheric Radiative Transfer of Sunshine: Algorithms and Performance Assessment*. Tech. Rep. FSEC-PF-270-95 [Available from Florida Sol. Energy Center, 1679 Clearlake Rd., Cocoa, FL 32922-5703].
- Gueymard, C. 1998. Turbidity determination from broadband irradiance measurements: a detailed multicoefficient approach. *J. Appl. Meteor.*, **37**, 414–435.
- Gueymard, C. and Kambezidis, H. 1997. Illuminance turbidity parameters and atmospheric extinction in the visible spectrum. *Q. J. Roy. Met. Soc.*, **123**, 679–697.
- Holben, B., Eck, T. F., Slutsker, I., Tanré, D., Buis, J. P., Setzer, A., Vermote, E., Reagan, J. A., Kaufman, Y. J., Nakajima, T., Lavenu, F., Jankowiak, I., and Smirnov, A. 1998. AERONET – a federated instrument network and data archive for aerosol characterization. *Remote Sens. Environ.*, **66**, 1–16.

- Ionov, D. V. 2010. Tropospheric NO₂ trend over St. Petersburg (Russia) as measured from space. *Russ. J. Earth Sci.*, **11**, ES4004, 1–7.
- Jakobson, E., Ohvril, H., Okulov, O., and Laulainen, N. 2005. Variability of radiosonde-observed precipitable water in the Baltic region. *Nordic Hydrol.*, **36**, 423–433.
- Jakobson, E., Ohvril, H., and Elgered, G. 2009. Diurnal variability of precipitable water in the Baltic region, impact on transmittance of the direct solar radiation. *Boreal Environ. Res.*, **14**, 45–55.
- Kalitin, N. N. 1938. *Actinometry*. Gidrometeorologicheskoe izdatelstvo, Leningrad–Moscow (in Russian).
- Kallis, A., Russak, V., and Ohvril, H. 2005. 100 years of solar radiation measurements in Estonia. In *Report of the 8th Session of the Baseline Surface Radiation Network (BSRN) Workshop and Scientific Review, Exeter, UK, 26–30 July 2004*. World Climate Research Programme, WMO, WCRP Informal Report No. 4/2005, March 2005, C1–C4.
- Kambezidis, H. D., Katevatis, E. M., Petrakis, M., Lykoudis, S., and Asimakopoulos, D. N. 1998. Estimation of the Linke and Unsworth–Monteith turbidity factors in the visible spectrum: application for Athens, Greece. *Sol. Energy*, **62**, 39–50.
- Kondratyev, K. Y. 1969. *Radiation in the Atmosphere*. Academic, San Diego, Calif.
- Lenoble, J. 1993. *Atmospheric Radiative Transfer*. A. Deepak, Hampton, Virginia, USA.
- Maurellis, A. and Tennyson, J. 2003. The climatic effects of water vapour. *Phys. World*, May, 29–33 (<http://physicsworld.com/cws/article/print/17402>).
- Myurk, Yu. Kh. and Okhvril, Kh. A. 1990. Engineering procedure for adjusting coefficient of atmospheric transparency from one atmospheric mass to another. *Soviet Meteorol. Hydrol.*, **1**, 89–95.
- Ohvril, H., Okulov, O., Teral, H., and Teral, K. 1999. The atmospheric integral transparency coefficient and the Forbes effect. *Sol. Energy*, **66**, 305–317.
- Ohvril, H., Teral, H., Tee, M., Russak, V., Okulov, O., Jõeveer, A., Kallis, A., Abakumova, G., Terez, E., Guschchin, G., Terez, G., Olmo, F. J., Alados-Arboledas, L., and Laulainen, N. 2005. Multi-annual variability of atmospheric transparency in Estonia. In *SOLARIS 2005, 2nd Joint Conference*. International Forum of Experts in Solar Radiation, Hellenic Illumination Committee, Athens, 42–46.
- Ohvril, H., Teral, H., Neiman, L., Kannel, M., Uustare, M., Tee, M., Russak, V., Okulov, O., Jõeveer, A., Kallis, A., Ohvril, T., Terez, E. I., Terez, G. A., Guschchin, G. K., Abakumova, G. M., Gorbarenko, E. V., Tsvetkov, A. V., and Laulainen, N. 2009. Global dimming and brightening versus atmospheric column transparency, Europe, 1906–2007. *J. Geophys. Res.*, **114**, 1–17.
- Okulov, O. 2003. *Variability of Atmospheric Transparency and Precipitable Water in Estonia During Last Decades*. PhD dissertation. Tartu University Press.
- Okulov, O. and Ohvril, H. 2010. *Column Transparency and Precipitable Water in Estonia. Variability During the Last Decades*. Lambert Acad. Publish., Saarbrücken, Germany.
- Okulov, O., Ohvril, H., and Kivi, R. 2002. Atmospheric precipitable water in Estonia, 1990–2001. *Boreal Environ. Res.*, **7**, 291–300.
- Olmo, F. J., Vida, J., Foyo-Moreno, I., Tovar, J., and Alados-Arboledas, L. 2001. Performance reduction of solar irradiance parametric models due to limitations in required aerosol data: case of the CPC2 model. *Theor. Appl. Climatol.*, **69**, 253–263.
- Peixoto, J. P. and Oort, A. H. 1992. *Physics of Climate*. American Institute of Physics.
- Smirnov, A., Holben, B. N., Eck, T. F., Slutsker, I., Chatenet, B., and Pinker, R. T. 2002. Diurnal variability of aerosol optical depth observed at AERONET (Aerosol Robotic Network) sites. *Geophys. Res. Lett.*, **29**(23), 2115, 30-1–30-4.
- Thomas, G. E. and Stamnes, K. 2002. *Radiative Transfer in the Atmosphere and Ocean*. Cambridge University Press.
- Toledano, C., Sorribas, M., Berjón, A., Morena de la, B. A., Frutos de, A. M., and Gouloub, P. 2007. Aerosol optical depth and Ångström exponent climatology at “El Arenosillo” AERONET site (Huelva, Spain). *Q. J. R. Meteorol. Soc.*, **133**, 795–807.
- Unsworth, M. H. and Monteith, J. L. 1972. Aerosol and solar radiation in Britain. *Q. J. R. Meteorol. Soc.*, **98**, 778–797.
- Veismann, U. and Eerme, K. 2011. *Solar Ultraviolet Radiation and Atmospheric Ozone*. Ilmamaa, Tartu (in Estonian).
- Zvereva, S. V. 1968. On the absorption of solar radiation by atmospheric water vapor. In *Actinometry and Atmospheric Optics. Reports of the Sixth Interdepartmental Symposium on Actinometry and Atmospheric Optics, June 1966, Tartu*. Valgus, Tallinn, 117–121 (in Russian).

Otsetee aerosooli laiaribaliselt optiliselt paksuselt spektraalsele

Martin Kannel, Hanno Ohvril ja Oleg Okulov

Nii Päikese laiaribalise ehk integraalse (kõiki lainepikkusi hõlmava) kui ka spektraalse otsekiirguse nõrgenemine atmosfääris on jaotatav kolmeks osaks: 1) hajumine ja neeldumine puhtas õhus ehk ideaalses atmosfääris, 2) neeldumine veeaurus, 3) neeldumine ja hajumine aerosooliosakeste (suuts, tolmu, udu) tõttu. Vastavalt on atmosfääri optiline paksus esitatav kolme optilise paksuse summana. Selle summa kaks esimest liiget, ideaalse atmosfääri ja veeauru optilised paksused, on arvutatavad, teades antud asukoha ideaalse atmosfääri koostist ning tegeliku atmosfääri niiskussisaldust antud vaatlushetkel. Summa kolmas liige, aerosooli optiline paksus, AOD (*aerosol optical*

depth), on eelmistega võrreldes väga muutlik. Kui aga atmosfääri kogu optiline paksus on Päikese otsekiirgusest määratud, saab sellest kahe komponendi, ideaalse atmosfääri ja veeauru optiliste paksuste lahutamise leida kolmanda ehk AOD.

Õhusambas sisalduvate aerosooliosakeste iseloomustamiseks on spektraalne AOD, eriti mõõdetuna mitmel lainepikkusel, oluliselt informatiivsem, kuid ka oluliselt kallim, võrreldes laiaribalisega – BAOD (*broadband aerosol optical depth*). Eestis alustati USA NASA programmi AERONET (Aerosol Robotic Network) raames ja selle programmi poolt finantseerituna Päikese otsekiirguse spektraalmõõtmisi 2002. aasta suvel Tõraveres. Sellest ajast alates täieneb unikaalne spektraalse AOD andmebaas Eesti kohal oleva atmosfääri kohta pidevalt.

Päikese integraalse otsekiirguse mõõtmisi alustati Eestis aga juba 1930. aastatel. Alates 1999. aastast kuulub Tartu-Tõravere ilmajaam ülemaailmsesse päikesekiirguse uurimise baasjaamade võrgustikku BSRN (Baseline Surface Radiation Network). Viimasel aastakümnel Tõraveres toimunud Päikese integraalse ja spektraalse otsekiirguse üheaegne registreerimine on loonud võimaluse uurida seoseid spektraalse ning integraalse AOD vahel.

Käesolevas töös on hinnatud ideaalse atmosfääri koostist Eesti kohal, esitatud valemid integraalse otsekiirguse neeldumiseks veeaurus ja koostatud ligi 20 000 vaatlusreast koosnev andmebaas spektraalse ning integraalse AOD ja õhusamba niiskussisalduse väärtustest Tõraveres aastatel 2002–2009. Selgus tihe paraboolne korrelatsioon spektraalse (500 nm) ja integraalse AOD vahel, mis võimaldas koostada üleminekuvalemi integraalselt AOD-lt spektraalsele. Kuna nimetatud valem on lihtne ega sisalda mingeid eeldusi õhus olevate aerosooliosakeste ei optiliste omaduste ega suurusjaotuste kohta, võib seda pidada 'otseteeks' (*shortcut*) üleminekul integraalsetelt spektraalsetele AOD väärtustele.

Üllatavalt andis meie tuletatud lihtne seos paremaid tulemusi kui Chr. Gueymardi koostatud ja senituntutest parim, kuid oluliselt komplitseeritud klassikaline mudel. Nimetatud keeruka mudeli mõnevõrra kehvemad tulemused on vähemalt osaliselt seletatavad Tõraveres kasutatava aktinomeetri (AT50) suurema avanurgaga (10°), võrreldes mujal levinud Eppley pürheliomeetriga ($5,7^\circ$), mis põhjustab Päikese oreoolikiirguse suuremat sisenemist mõõteriista ja tekitab mulje atmosfääri paremast läbipaistvusest.

Esitatud 'otsetee' integraalsetelt spektraalsetele AOD väärtustele võimaldab edaspidi kolme liiki rakendusi: 1) spektraalse AOD hinnanguid Tõraveres enne 2002. aastat, kui Päikese spektraalset otsekiirgust veel ei mõõdetud, 2) spektraalse AOD hinnanguid muudes meteojaamades ja ekspeditsiooniolukorras, kus piirduakse vaid integraalse otsekiirguse mõõtmistega, näiteks Tiirikoja järvejaamas, 3) automaatselt registreeritud spektraalse AOD aegridade kontrolli, kui on tekkinud kahtlus valguskiirt ekraneeriva takistuse (putukas, praht, suits lähipiirkonnas jne) sattumisest mõõteriista vaatevälja.